32nd URSI GASS, Montreal, 19–26 August 2017

Advanced multiple input multiple output (MIMO) SAR algorithm for high-resolution 3D reconstruction imaging

Xia Wu
School of Electronics and Information Engineering, Tongji University, 201804, Shanghai, P. R. China

Abstract

In this paper, an advanced multiple input multiple output (MIMO) SAR algorithm for high-resolution three-dimensional reconstruction imaging was proposed. Firstly, we give a short overview of the principle of scattering mechanism and the formulations of optimized physical optics (PO). Additionally, a three-dimensional(3D) MIMO SAR array is illustrated. Finally, NVIDIA's Compute Unified Device Architecture (CUDA) is used to parallelize and accelerate the Electromagnetics (EM) simulation and imaging process in a Graphics Processing Unit (GPU). An electrically-large target, Airbus A380, was computed and the 3D reconstruction image was presented.

Keywords: MIMO SAR, electrically-large, radar imaging, numerical calculation.

1 Introduction

A conventional radar system is Single-Input Single-Output (SISO) which can determine the relative distances and velocities of the targets. Furthermore, Single-Input Multiple-Output (SIMO) radar system with a single transmit antenna and multiple receive antennas can obtain two-dimensional reconstruction imaging results.

However, there is currently no effective method for three-dimensional complex targets based on electromagnetic scattering studies. In the literature, because of the complexity of the issue, most of the research focuses on analysis of simple shapes (such as spheres, cubes and cylinders), which leaves a wide gap between the model and the complex real scene.

Moreover, the national security and economy motive us to develop Synthetic Aperture Radar (SAR) imaging under Multiple-Input Multiple-Output (MIMO) architecture, which is a frontier research area in radar imaging for 3D reconstruction imaging. For radar applications, MIMO is a relatively new technology. RIAS was invented by ONERA in 1989 and a sparse-array synthetic impulse and aperture radar (SIAR) proposed by National Lab of Radar Signal Processing of Xidian University. They can be seen as the prototype of MIMO radars [1, 2]. From 2006, a research group in Germany started to develop ARTINO 3D imaging SAR by using a MIMO Array [3].

In my previous work, the numerical solution of Single-Input Multiple-Output (SIMO) radar imaging, by combining the Fast Back Projection (FBP) method was proposed [4]. As an extension research of SIMO SAR, the MIMO SAR architecture possesses various advantages in terms of signal-to-noise ratio of receiving signals, as well as target detectability.

2 Principle of Scattering Mechanisms

Optimized PO method can be used for scattering analysis. Hereby, we define f_c is the carrier frequency. Note that the wave number $k = 2\pi f_c/c$, $\hat{d}_i$ is the unit vector in the direction of propagation of the incident wave. The incident plane wave is given by Equation (1) as following

$$\vec{E}_i(\vec{r}) = \vec{E}_{i0} e^{-jk(\hat{d}_i \cdot \vec{r})}, \quad \vec{H}_i(\vec{r}) = \vec{H}_{i0} e^{-jk(\hat{d}_i \cdot \vec{r})}. \tag{1}$$

in which $\vec{E}_{i0}$ depends on the direction of polarization of the incident wave, $\vec{H}_{i0} = (\mu_0 c)^{-1} \hat{d}_i \times \vec{E}_{i0}$.

For a given target, the far-field scattering properties was calculated for specified direction with respect to $\hat{d}_s$, the unit vector in the direction of propagation of the scattering wave. Assuming that S represents the target surface, and for $\vec{r'} \in S$, $\hat{n}$ is the unit normal vector. If $\vec{r'}$ is directly irradiated by the incident wave, where the surface current density $\vec{J}_s(\vec{r})$ can be approximated as

$$\vec{J}_s(\vec{r'}) \approx 2(\hat{n} \times \vec{H}_{i0}) e^{-jk(\hat{d}_i \cdot \vec{r'})}. \tag{2}$$

For the $\vec{r'}$ in the shadowing, the existence of phase stagnation in the surface integral lead to $\vec{J}_s(\vec{r})$ can be approximated as zero.

Considering that only a part of S can be irradiated by the incident wave, which we denote as S_1. For electrically-large targets, in particular, an airplane model including a variety of large planes, we wish to realize an optimized algorithm, this permits the integral of Equation (3) can be calculated directly in arbitrary size of triangle $\mathscr{A}$ in S_1.

$$\vec{H}_s(\vec{r}) = -\frac{e^{-jkr}}{4\pi r} \sum_{\mathscr{A} \subseteq S_1} 2jk(\hat{d}_s \times (\hat{n} \times \vec{H}_{i0}) I(\hat{d}_s - \hat{d}_i; \mathscr{A}). \tag{3}$$

$$\vec{E}_s(\vec{r}) = -\frac{1}{\varepsilon_0 c}(\hat{d}_s \times \vec{H}_s(\vec{r})). \quad (4)$$

$$I(\hat{d};\mathscr{A}) = \int_{\mathscr{A}} dS(\vec{r'}) e^{-jk(\hat{d}\cdot\vec{r'})}. \quad (5)$$

3 3D MIMO SAR Array

A MIMO array with N_{Tx} transmit and N_{Rx} receive antennas was considered, see Figure 1 for an illustration, where N_{Tx} and N_{Rx} are the number of transmitters and receivers. Here T_x and R_x correspond to transmit antennas and receive antennas, respectively. The d_{inc} and $d_{scatter}$ in the figure are the direction of incident and scattering, that is, taking the spherical coordinate system into account, the transmit antennas (T_x) are uniformly spaced in half xz-plane with $\phi = 0$ and $\theta \in [\frac{\pi}{6}, \frac{5\pi}{6}]$ and point to the target. Similarly, the receive antennas R_x are uniformly spaced in half yz-plane with $\phi = \frac{\pi}{2}$ and $\theta \in [\frac{\pi}{2}, \frac{3\pi}{2}]$, outward to the target.

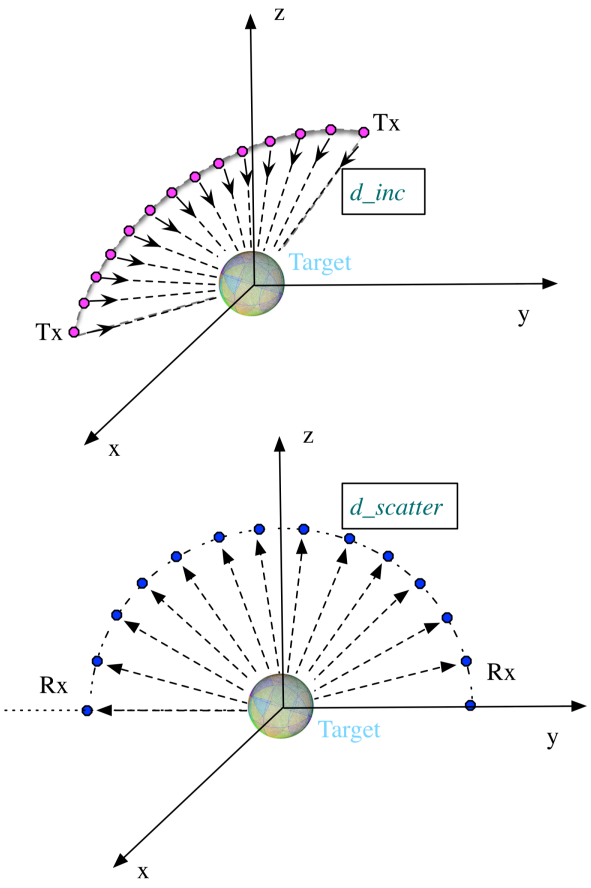

Figure 1. Principle of MIMO radar system: purple and blue circles correspond to transmit and receive antennas.

In this work, we assume that the target is located in the far field of the MIMO array, i.e., the distance of the target to the transmitters and receivers should be sufficiently large enough to satisfy the far field condition. As a consequence, except for a common factor, $e^{-jkr}/4\pi r$, $\vec{E}_s(\vec{r})$ in Equation (4) is a function of $\hat{d}_s$, $\hat{d}_i$ and k. $\hat{d}_s$ and $\hat{d}_i$ are the direction of scattering and incident, respectively. Taking the dot product of vector of polarization direction by scattering, the integral value is possible that as a result of the far-field scattering imaging.

4 Hardware Acceleration for Fast Computation

The computation was carried on a computer workstation with configuration of NVIDIA's Compute Unified Device Architecture (CUDA), 256 GB memory for original solver. The parallel experimental platform based on the GK110 core Tesla K20, GK110 has up to 2,496 stream processors (CUDA) and double-precision floating-point operation speed of 1.4-1.5T FLOPS (floating point operations per second) [5]. By using the GPU hardware system, it could substantially speed up the above-mentioned MIMO SAR imaging algorithm to achieve real-time imaging.

5 Geometric Modelling and 3D SAR Imaging

5.1 Geometric Modelling

The first simple case is a metal sphere of radius $R = 1.0$ meter. Hereby, Gmsh, a three-dimensional finite element grid generator with a build-in CAD engine and post-processor is utilized. It can provide a fast, light and user-friendly meshing tool with parametric input [6]. Gmsh plots graphs of mesh quality parameters and Figure 2 shows the statistics window, there are 29 points, 56 lines and 32 surfaces in Sphere.geo.

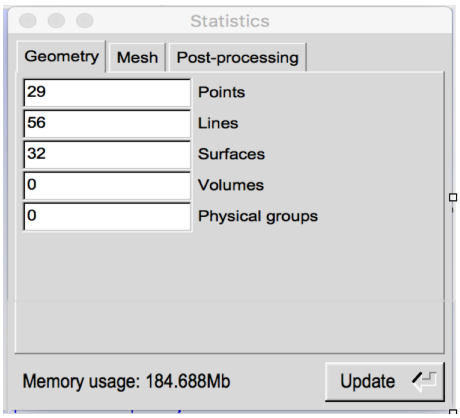

Figure 2. Gmsh parameter statistics of Sphere.geo.

The second case is a commercial aircraft, Airbus A380, the model contains the main body with overall length of 72.72 meters, the wingspan of 79.75 meters and the height of 24.09 meters including four engines. The original geometry version is A380.geo. The mesh generation is performed in the Figure 3. Figure 4 shows that the geometric model including 88489 points, 258588 lines and 172117 surfaces.

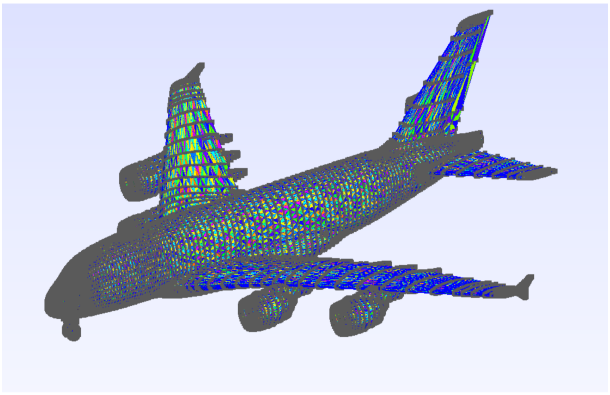

Figure 3. 3D mesh of Airbus A380 generated by Gmsh.

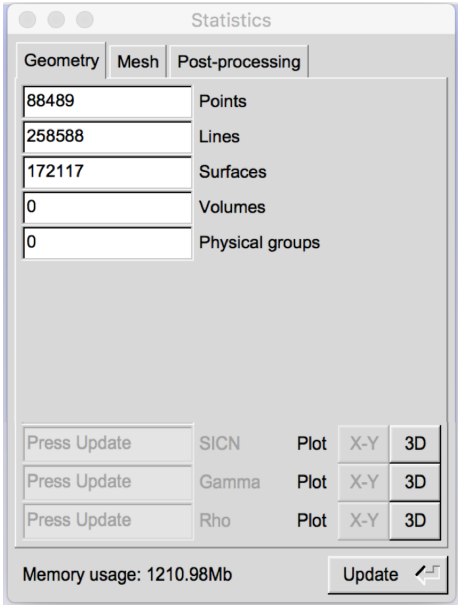

Figure 4. Gmsh parameter statistics of Airbus A380.geo.

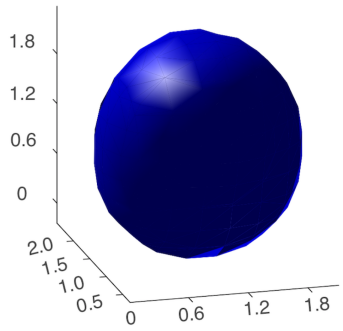

Figure 5. The SAR imaging of Sphere (3D).

5.2 3D SAR Imaging

For different $\vec{r}$, by employing Maximum Intensity Projection (MIP)[7], a more realistic three-dimensional shape of the target is reconstructed in presentation of the scattering field data $\vec{E}_s(\vec{r})$.

3D MIMO SAR imaging of the sphere and the Airbus A380 are shown in Figure 5 and Figure 6, respectively. Obviously, the reconstruction of sphere model in Figure 5 demonstrated that the proposed MIMO SAR imaging algorithm is correct based on reliable computation. It can be seen from Figure 6 that the main body of Airbus A380 model including the wingspan and four engines are clearly reconstructed as well. Table 1 illustrated the parameters of two numerical cases and run time.

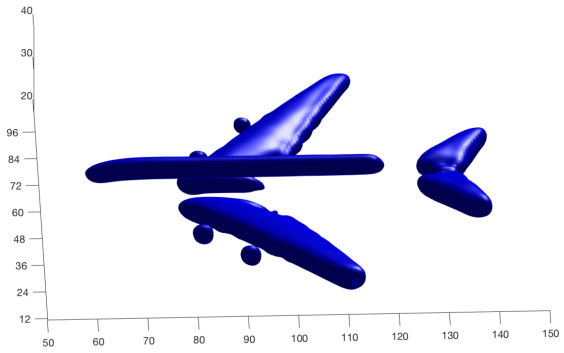

Figure 6. The SAR imaging of A380 (3D).

Table 1. The parameters: N_{Tx} , N_{Rx} and sweep frequencies Vs Run time.

Numerical case	N_{Tx}	N_{Rx}	Low freq. (MHz)	High freq. (MHz)	Run time (second)
Sphere	65	65	125	250	2.99
A380	193	193	375	750	183.65

6 Conclusion

As an emerging field, the realization of MIMO SAR still faces many challenges. Especially for the huge computation consumption caused by the electrically large scale targets in processing of 3D radar imaging. According to the simulation results of two numerical cases, the reported MIMO SAR 3D imaging system is demonstrated to achieve the goal of providing real-time 3D reconstructions of radar imaging. One of the important applications of MIMO SAR is on high-resolution microwave imaging, a technology which can connect to a huge varieties of emerging industries including airport security checks as well as auto piloting. The two aforementioned industry applications represent future potentials of radar techniques.

7 Acknowledgements

This work was supported by the Shanghai Natural Science Foundation (Grant No. 16ZR1446300).

References

[1] J. Dorey, G. darnier, G. Auvray, "RIAS, synthetic impulse and antenna radar," *International Conference on Radar*, Paris, 1989, pp. 556–562.

[2] B.X. Chen, S.H. Zhang, Y.J. Wang and J. Wang, "Analysis and experimental results on sparse-array synthetic impulse and aperture radar," *Proceedings of 2001 CIE International Conference on Radar*, 2001, pp. 76–80.

[3] J. Ender and J. Klare, "System architectures and algorithms for radar imaging by MIMO-SAR," *IEEE Radar Conference*, Pasadena, CA, May 2009.

[4] X. Wu and Y.Q. Jin, "Scattering Model for Electrical-Large Target Employing MLFMA and Radar Imaging Formation," *Journal of the Korean Institute of Electromagnetic Engineering and Science*, **10**, 3, September 2010, pp. 166–170.

[5] "Tesla K20 GPU Accelerator," *Nvidia.com*, Retrieved 2015-12-11.

[6] C. Geuzaine and J.F. Remacle, "Gmsh: a Three-Dimensional Finite Element Mesh Generator with Built-in Pre- and Post-processing Facilities," http://www.geuz.org/gmsh/, May, 2004.

[7] J.W. Wallis, T.R. Miller, "Three-dimensional display in nuclear medicine and radiology," *Journal of Nuclear Medicine*, **32**, 3, March 1991, pp. 534–546.